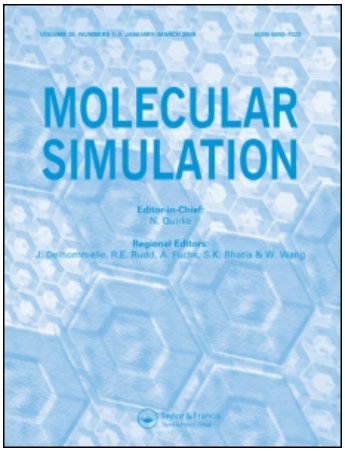

Molecular Simulation
Publication details, including instructions for authors and subscription information:
http://www.informaworld.com/smpp/title~content=t713644482

Force field comparisons of the heat capacity of carbon nanotubes

C. Y. Guo[a]; B. Montgomery Pettitt[b]; L. T. Wheeler[a]
[a] Mechanical Engineering, University of Houston, Houston, TX, USA [b] Chemistry, University of Houston, Houston, TX, USA

To cite this Article Guo, C. Y. , Pettitt, B. Montgomery and Wheeler, L. T.(2006) 'Force field comparisons of the heat capacity of carbon nanotubes', Molecular Simulation, 32: 10, 839 — 848
To link to this Article: DOI: 10.1080/08927020600962956
URL: http://dx.doi.org/10.1080/08927020600962956

Molecular Simulation, Vol. 32, Nos. 10–11, 30 August–15 September 2006, 839–848

Taylor & Francis
Taylor & Francis Group

Force field comparisons of the heat capacity of carbon nanotubes

C. Y. GUO†, B. MONTGOMERY PETTITT‡* and L. T. WHEELER†

†Mechanical Engineering, University of Houston, Houston, TX 77204-4006, USA
‡Chemistry, University of Houston, Houston, TX, 77204-5003 USA

(Received July 2006; in final form August 2006)

The force fields Tersoff, CHARMM, COMPASS, CVFF and PCFF are compared using molecular calculations and simulations of SWNT thermal properties. The heat capacity results from the force fields vary significantly in the low (room) temperature range. The COMPASS force field best reproduces the phonon frequencies calculated from density functional theory and is consistent with the Raman scattering results. The temperature dependent behavior of SWNT heat capacity is investigated using harmonic and quasi-harmonic dynamics theories. The impact of quasi-harmonic analysis is not significant in the low and intermediate temperature range (below 500 K). Thus, force field comparisons based on the harmonic approximation are valid in that temperature range. Above 500 K, heat capacity results based on the Tersoff force field using a quasi-harmonic approximation are further investigated.

Keywords: Quasi-harmonic; Nanotubes; Molecular mechanics; Molecular dynamics

1. Introduction

Since the discovery of single walled carbon nanotubes (SWNTs) in 1991 [1], a significant number of investigations have studied the mechanical and electronic properties of SWNTs and multi-walled carbon nanotubes (MWNTs). In contrast, investigation into the thermal properties of nanotubes has not received the same attention, either experimentally or computationally. In this paper we take a molecular simulation approach to the problem of the relationship of the force field functional form and parameters to the predicted heat capacities for two kinds of SWNTs.

Hone *et al.* [2,3] measured the isobaric specific heat of SWNTs and found the measured value agrees with a prediction for individual nanotubes and is significantly smaller than that of graphene below 50 K. The specific heat of a bundle of MWNTs was obtained in an experiment by Yi [4] concerned with the measurement of the thermal conductivity of this system. The results demonstrate a strikingly linear temperature-dependent specific heat over the entire temperature range measured (10–300 K). Recently, the specific heat of SWNT bundles was measured down to 0.1 K [5]. Due to the uncertainty in the composition of nanotube samples, it is difficult to understand the measured thermal properties in terms of specific nanotubes accurately. Computer simulations play an important role therefore in the study of the thermal properties of nanotubes.

Molecular mechanics (MM), molecular dynamics (MD) and density functional theory (DFT) are three methods available for simulating the thermal properties of SWNTs and MWNTs. Due to the computationally intensive nature of electronic structure calculations like DFT, the other two methods are more widely used. In MM and MD, force field selection is critical to the validity of simulation results. In the literature, many force fields are used for investigation of the physical properties of carbon nanotubes. Saito *et al.* [6] adopted tight-binding MD for the nanotube geometry and used the general atomic force field for carbon materials to calculate the phonon frequency and raman intensity of SWNT. Porter [7] used the Tersoff force field to obtain the harmonic and quasi-harmonic frequencies of silicon carbide. Rao *et al.* [8] used the force constant method to calculate the vibrational models in carbon nanotubes and compared the Raman scattering active modes. Prylutskyy [9] used a simple self defined force field to calculate the vibrational properties of SWNT.

*Corresponding author. Email: pettitt@uh.edu

Molecular Simulation
ISSN 0892-7022 print/ISSN 1029-0435 online © 2006 Taylor & Francis
http://www.tandf.co.uk/journals
DOI: 10.1080/08927020600962956

Sokhan *et al.* [10] calculated the phonon spectra of carbon nanotube using Tersoff–Brenner force field, and Longhurst and Quirke [11,12] studied radius dependent behavior and the environmental effect on the radial breathing modes of SWNTs using the second generation reactive empirical bond order potential (REBO) [13]. The Tersoff type force field has been very successful in mechanical property simulation of carbon nanotubes, but is unproved in thermal properties simulations. The CHARMM force field [14,15,16] is widely used in the MD simulation of protein and DNA. CVFF [17] and PCFF [18] force fields developed by Accelrys are designed to improve the vibrational analysis of molecules. The proprietary COMPASS [19,20] force field incorporates recent DFT results and fits parameters with the aid of experimental data.

The aim of the present article is to assess the quality of various empirical force fields by simulating the heat capacity of the SWNTs, and compare the results with those of DFT and available experimental results. The temperature dependent nature of phonon frequencies and their impact on heat capacity are also investigated. The following force fields are evaluated: Tersoff, CHARMM, CVFF, PCFF and COMPASS.

2. Method

We used harmonic and quasi-harmonic calculations to test and compare the different force fields. We begin with a brief overview of the potentials. More complete descriptions are available in the extensive literature for each.

2.1 Empirical force fields

The total energy of a molecule can be approximated as the sum of individual force field terms,

$$E = E_{\text{bond}} + E_{\text{angle}} + E_{\text{torsion}} + E_{\text{oop}} + E_{\text{cross}} + E_{\text{nonbond}}. \quad (1)$$

The bond, angle and torsion terms are self explanatory. The E_{oop} describes out-of-plane bonding interactions, and the E_{cross} describes the interaction between bond, angle and torsion terms. The non-bonded terms consist of excluded volume, dispersion and electrostatic parts and are given by E_{nonbond}.

All force fields in the test include the bond and angle terms. Some force fields also add the torsion, cross and out-of-plane terms. Except for Tersoff, the force fields tested here also include the non bonded terms. The non bonded part is defined differently in each force field (See below). While the same expression employing the atom-centered point charges is used for the electrostatic term, none of the force fields used explicitly include the polarization term.

2.1.1 Tersoff-type many-body hydrocarbon force field. The Tersoff [21] force field for hydrocarbons can model the single, double and triple carbon—carbon bonding in a variety of small hydrocarbon molecules as well as in diamond and graphite. In this model, the energy is written as

$$E = \frac{1}{2}\sum_i \sum_{i \neq j} f_c(r_{ij})\left[V^R(r_{ij}) + b_{ij}V^A(r_{ij})\right], \quad (2)$$

where r_{ij} is the atomic distance, $f_c(r_{ij})$ is the cutoff function, $V^R(r_{ij})$ represents the repulsion part and $V^A(r_{ij})$ represents the attraction part. The many body features of the potential are hidden in the bond-order function b_{ij}, between atoms i and j, which depend on the local atomic environment in which a particular bond in located. All many-body effects, such as changes in the local density of states with varying local bonding topologies, are approximately included in this term. The Tersoff force field is characterized as a nearest neighbor potential. Based on the Tersoff force field, Brenner presented a potential [22] that can model the bonding situations intermediate between single and double bonds due to bond conjugation. Since this potential was too restrictive to simultaneously fit equilibrium distances, energies and force constants for carbon—carbon bonds, Brenner *et al.* later developed a second-generation REBO potential [13] which includes both improved analytic functions for the intra-molecular interactions, as well as an expanded fitting database.

2.1.2 CHARMM. The Chemistry at HARvard Macromolecular Mechanics (CHARMM) program with empirical energy function parameter set 27 [15,16] is used. The CHARMM model [14] was designed for large macromolecules. It includes bonds, angles, torsion and out-of-plane terms. The van der Waals (vdW) interactions in CHARMM 30b1 are described with a 6–12 potential. The vdW parameters are obtained from experimental geometries, *ab initio* interaction energies and from heats of sublimation of some analogs.

2.1.3 CVFF. The consistent-valence force field (CVFF) [17] was designed for materials science applications. It is extensively used for describing crystals formed from small molecules. It is the original force field in the DISCOVER module of the Accelrys program [23]. The pair potential is a Morse-potential. The CVFF also include the torsion term and the cross term between bond and angle. The vdW term is described with a 6–12 potential.

2.1.4 PCFF. The Polymer Consistent force field (PCFF) [18], designed by Accelrys [23] to improve the vibrational analysis of molecules, is a second generation force field. It fits a large number of chemical compounds, including the elements H, C, N, etc. and some parameters have also fit data derived from Hartree-Fock calculations. In addition

to the quadratic term approximation for bonds and angles, PCFF includes the third and fourth order approximation terms. It also includes the cross terms among energies corresponding to bond, angle and torsions. The vdW term is described with a 6–9 potential.

2.1.5 COMPASS. The Condensed-phase Optimized Molecular Potentials for Atomistic Simulation Studies (COMPASS) [19,20] is based on the PCFF force field and its earlier versions. In contrast to earlier force fields that were developed with an emphasis on predicting the structure of isolated molecules or pairs of molecules in gas phases, COMPASS is an *ab initio* based force field parameterized using extensive data for molecules in condensed phases.

2.2 Heat capacity calculation

The isometric heat capacity of a system, C_v, measures how the internal energy responds to an isometric change in temperature, and is expressed as [24]

$$C_V = k_B \sum_{\mathbf{k},\nu} \left[\frac{\hbar\omega(\mathbf{k},\nu)}{k_B T}\right]^2 \frac{e^{(\hbar\omega/k_B T)}}{\left[e^{(\hbar\omega/k_B T)} - 1\right]^2}, \qquad (3)$$

where k_B is the Boltzman constant, $\hbar$ is the Plank constant, and ω is the phonon frequency. Here $\mathbf{k}$ is the wave vector, which lies in the brillioun zone and labels the mode of the phonon frequency.

In the harmonic approximation, ω is independent of temperature. The C_V is valid at temperature ranges below the Debye temperature θ. Above the Debye temperature, the anharmonic effects must be included to account for the temperature dependent behavior of phonon frequency. The vibrational heat capacity C_{vib} is expressed as:

$$C_{\text{vib}} = k_B \sum_{\mathbf{k},\nu} \left[\frac{\hbar\omega(T,\mathbf{k},\nu)}{k_B T}\right]^2 \frac{e^{(\hbar\omega/k_B T)}}{\left[e^{(\hbar\omega/k_B T)} - 1\right]^2}. \qquad (4)$$

The temperature dependent phonon frequencies are computed from the weighted fluctuation matrix at the temperature specified for the MD simulation.

3. Results and discussion

We calculate the heat capacity of armchair (5,5) and (10,10) isolated SWNTs based on the harmonic lattice dynamics (HA) and quasi-harmonic lattice dynamics (QHA) methods. Besides local codes, the atomic simulation module in Materials Studio [23] and the MD simulation program CHARMM are used in the computation. The results are described in detail in the following sections.

3.1 Harmonic lattice dynamics (HA)

The phonon modes and frequencies of SWNT are obtained by harmonic analysis. From formula (3), the quality of the heat capacity is determined by the quality of the phonon density of states (PDOS). The lower rather than the higher, phonon frequencies contribute more to the heat capacity, and are the dominant factor in the low temperatures. Jishi *et al.* [25,26] used the force constant method to calculate the zone-folding phonon frequencies of SWNT. Rao *et al.* [8], Richter [27], Saito [6] and Maeda [28] used force constants fitted to graphite, and Charlier [29] modified force constants to account for the curvature of the tube in calculating the harmonic phonon frequencies of the tube. Popov [30,31] used the valence force field and parameters of graphite to obtain the harmonic phonon frequencies. Sanchez-Portal *et al.* [32] used DFT (local density approximation) to get a more accurate description of the phonon density of the states. Sokhan *et al.* [10] studied the phonon spectra of carbon nanotube using Tersoff–Brenner force field and compared the RBM frequencies with force constant, *ab initio* and tight-binding calculations. All results on phonon frequencies are based on SWNT with periodic boundary conditions (PBC). The models in the force constant method fix the C—C bond length, and assume that the SWNT always keeps the original symmetry of the unit cell. This rules out the possibility of structural optimization of the tube.

In this article, we use the aforementioned force fields to calculate the potential energy of the initial SWNT configuration. The SWNT is relaxed to the equilibrium configuration by minimizing the total energy. Based on harmonic theory, the phonon frequencies of the minimized SWNT configurations are calculated. Since some force fields consider the torsion, cross and out of plane terms, the minimized structure may deviate slightly from the original perfect symmetry. For comparison, we first calculated the phonon frequencies of a isolated SWNT with axial PBC, then we calculated the phonon frequencies of a finite length, H-terminated SWNT which reveals more vibrational modes along the axial direction.

3.1.1 Infinite length SWNT. A SWNT with axial PBCs can simulate an isolated infinite length SWNT. The unit cells used for simulation are shown in figure 1. There are 20 carbon atoms in the (5,5) SWNT unit cell and 40 carbon atoms in the (10,10) SWNT unit cell.

Phonon Frequency Comparison. We calculated the phonon frequencies of the SWNT unit cell at the Γ point. There are 60 frequencies for a (5,5) SWNT and 120 frequencies for a (10,10) SWNT. Tables 1 and 2 list only a few of the lowest and highest frequencies of SWNT based on different force fields. Since the CHARMM program does not support vibration analysis of molecules with PBCs, only the results from COMPASS, Tersoff, PCFF, CVFF are shown in the tables. The breathing mode with A_{1g} symmetry is the signature mode of the SWNT.

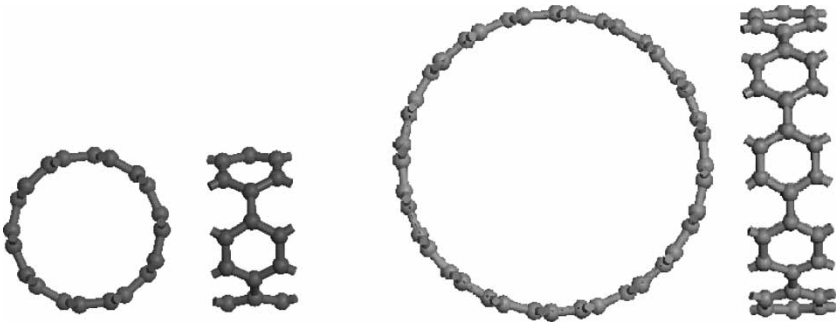

Figure 1. (a). (5,5) SWNT-20 atoms (b). (10,10) SWNT—40 atoms.

The results from DFT (marked as S–P) [32] and the force constant method (marked as JiShi) [26] are also shown in the tables. We also show the first-order Raman-active vibrational mode frequencies (marked as Raman) based on an ensemble of $n = 8-11$ armchair (n, n) nanotubes [8].

Except for CVFF, the highest frequencies of COMPASS, Tersoff and PCFF are very close, and differ by no more than 6%. But this is not the case for the lowest frequencies. For the lowest E_{2g} mode, the Tersoff force field gives a very high $142\,\mathrm{cm}^{-1}$ for (10,10) SWNT and $228\,\mathrm{cm}^{-1}$ for (5,5) SWNT, which are well above the values calculated by the other three force fields and the force constant method. In the four lower Raman-active vibrational modes E_{1g}, A_{1g}, E_{2g}, A_{1g} for (10,10) SWNT, the frequencies calculated from the COMPASS force field match almost perfectly to that of the Raman Scattering results. In light of the lowest A_{1g} breathing mode, the frequency (10,10) SWNT from DFT is $172\,\mathrm{cm}^{-1}$, the deviations from DFT result are respectively 4, 1, 9.5, 16.4 and 26.7% for Force-constant, COMPASS, Tersoff, PCFF and CVFF. The frequency from Raman is $186\,\mathrm{cm}^{-1}$, which is higher than the frequency from DFT. The reason is that frequencies from Raman experiments are based on an ensemble of $n = 8-11$ armchair (n, n) nanotubes. The results of the lowest A_{1g} breathing mode is similar for the (5,5) SWNT. We conclude that for the SWNT with PBC's, the COMPASS force field gives the best predictions of the vibrational modes among the force fields used.

The fact that the COMPASS force field is superior to the PCFF and CVFF force fields may be attributed to the parameters which incorporate *ab initio* calculations adjusted for molecules in the condensed phase. Why COMPASS performs better than the popular Tersoff force field is allusive at first. After comparison of these two force fields, we find the following influencing factors:

1. The COMPASS force field includes the additional torsion, out-of-plane and bond-angle cross terms which are beneficial in describing the vibration modes of nanotube molecules.
2. The COMPASS force field includes the non-bond terms such as vdW and coulomb forces, while the Tersoff force field considers only its nearest neighbors due to the cutoff function.
3. In the temperature range where harmonic lattice dynamics is valid, there is no bond breaking or formation, the conjugate number for each of the carbon atoms remains the same. Both the COMPASS and Tersoff force fields simulate partial bonds and bond breaking which is not required at low temperatures.

Heat Capacity Comparison. According to equation (3), the heat capacity of SWNTs is obtained from the phonon frequencies. The results are shown in figures 2–4. For (10,10) SWNTs, all force fields predict similar heat capacities in the high temperature range ($>1500\,\mathrm{K}$), which agrees with the expectations of classical statistical mechanics. Results show that heat capacity is not sensitive to the force field at high temperatures. In the medium temperature range (300–1500 K), PCFF (dash-dot line) predicts the highest heat capacity, while CVFF (dotted line) predicts the lowest. At room temperature 300 K, the heat capacity for PCFF (733.37 J/Kg/K) is twenty percent higher than the heat capacity for CVFF (611.10 J/Kg/K),

Table 1. (5,5) SWNT phonon frequencies (cm^{-1}) at Γ point.

Mode	*S–P*	*Jishi*	*COMPASS*	*Tersoff*	*PCFF*	*CVFF*
E_{2g}			81	228	58	71
E_{1g}			198		206	270
A_{1g}	340	311	345	302	395	444
Highest			1952	1901	1823	2227

Table 2. (10,10) SWNT phonon frequencies(cm^{-1}) at Γ point.

Mode	*Raman*	*S–P*	*Jishi*	*COMPASS*	*Tersoff*	*PCFF*	*CVFF*
E_{2g}			22	27	142	9	21
E_{1g}	116		117	99		105	136
A_{1g}	186	172	165	170	156	200	218
E_{2g}	377		368	378		432	243
E_{2g}	377		371	378		432	243
A_{1g}	673		670	678		748	839
Highest	1680			1976	1953	1883	2251

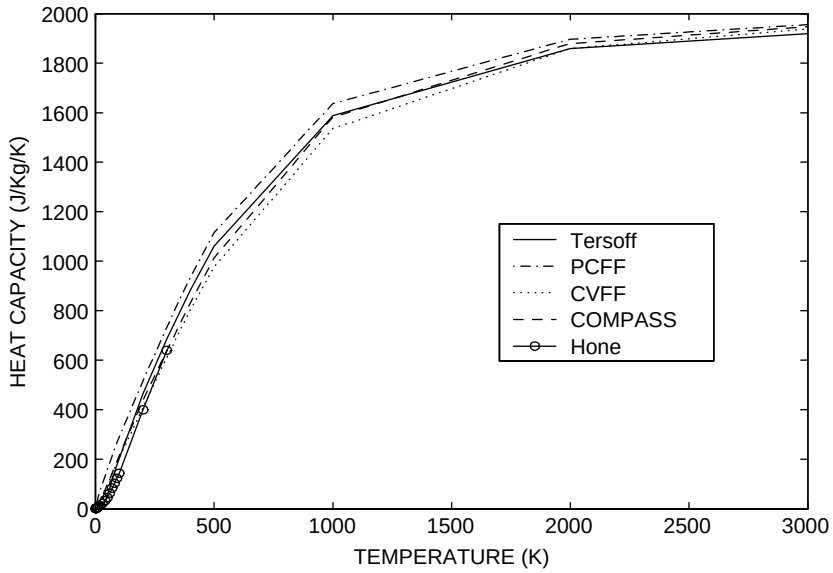

Figure 2. (10,10) SWNT PBC heat capacity from 0 to 3000 K.

which shows the influence of the force field. In the low temperature range (<300 K), the difference in heat capacity for different force fields becomes more significant. The measured heat capacity of SWNTs [3] up to 300 K is also shown (solid line with circle mark). PCFF test results show the largest deviation. At a temperature of 50 K, the heat capacity for PCFF(158.39 J/Kg/K) is three times higher than the experimental result (45 J/Kg/K). The Tersoff (solid line) results agree well with the experimental results in the temperature range near 50 K. COMPASS (dashed line) and CVFF results show small deviations from the experimental results in the temperature range below 10 K and above 100 K. In the low temperature range, the heat capacity from all the force fields shows a nearly linear dependence on temperature, which is confirmed by Benedict [33]. The heat capacity results of (5,5) SWNTs show similar behavior for the force fields as that of (10,10) SWNTs.

3.1.2 Finite length SWNT. Since SWNTs with the PBC model did not capture some of the vibrational modes along the axial direction, we also investigated finite length SWNT models. We use 360 atoms in each (5,5) and (10,10) SWNT finite length models. The hydrogen atoms are added at the end of the SWNTs for chemical stability.

Phonon Frequency Comparison. We calculated the phonon frequencies of (5,5) and (10,10) finite length SWNTs. Table 3 lists the five lowest and highest

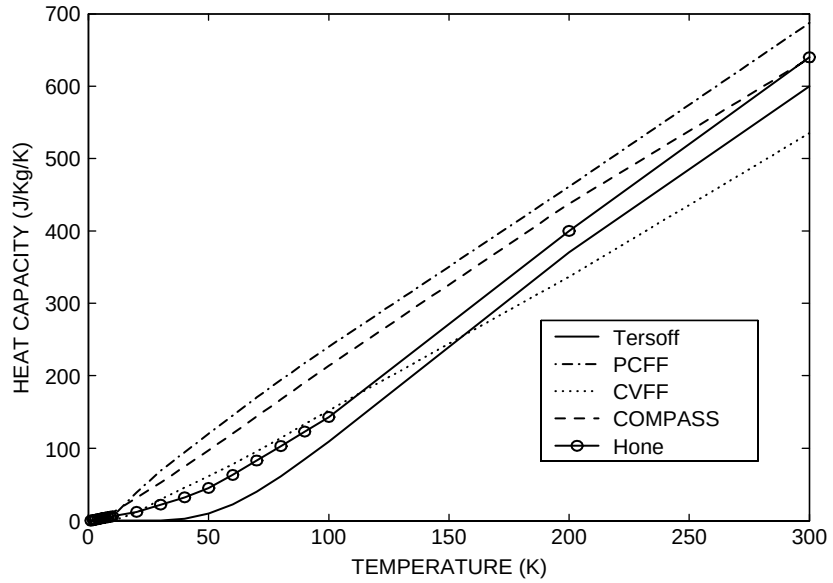

Figure 3. (10,10) SWNT PBC heat capacity from 0 to 300 K.

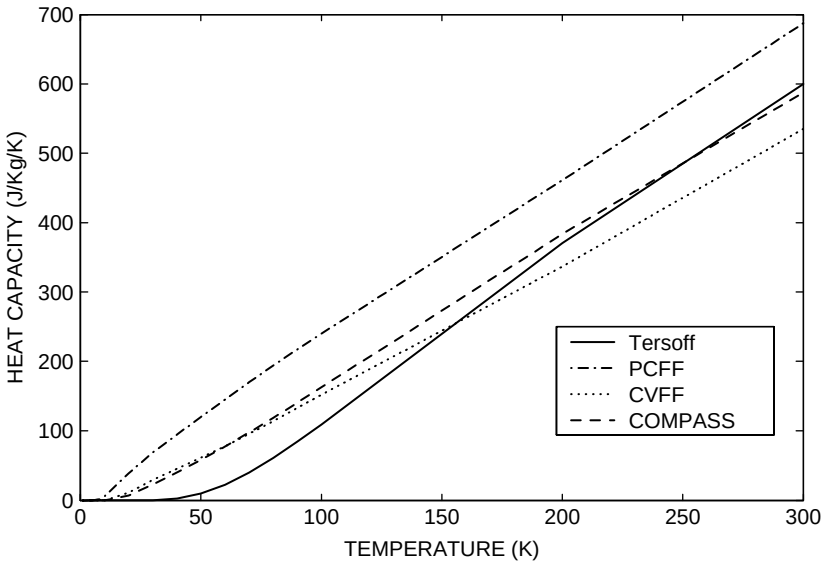

Figure 4. (5,5) SWNT PBC heat capacity from 0 to 300 K.

frequencies of the SWNTs based on the different force fields. The six frequencies corresponding to the translation and rotation of whole SWNTs are not shown, and the ultra high frequencies caused by the hydrogen at each end are also eliminated. Compared to the results of SWNT with PBCs, the value of the lowest and highest frequencies is smaller. This confirms that the finite length SWNT configuration is softer due to the removal of the constraint imposed by the PBCs along the axial direction. The PDOS are shown in figures 5 and 6.

Heat Capacity Comparison. The heat capacity of finite length SWNTs is obtained from the PDOS results and shown in figures 7–9. Like the case for SWNTs with PBCs, the heat capacity results are not sensitive to the force field in the high temperature range. In the low temperature range (below 300 K), the Tersoff force field shows the highest heat capacity values, while the CVFF force field shows the lowest for (10,10). The heat capacity values calculated from the CHARMM force field have the least deviation from the experimental results of SWNTs [3]. The COMPASS force field has smaller deviations than the Tersoff force field.

3.2 Quasi-harmonic lattice dynamics (QHA)

Since harmonic phonon frequency can not capture the temperature dependence, the heat capacity results discussed in the last section are only valid up to the Debye temperature. To obtain the temperature dependent phonon frequency spectrum, MD simulation is used to heat up the SWNT configuration to the specified temperature. The NPT ensemble is used and a Nosé heat bath [34,35] is specified. After the SWNTs are stabilized at the specified temperature, we record the fluctuations and positions of the atoms for a period of 10^6 timesteps(each timestep is 1 fs). Table 4 shows the heat capacity values change with increased simulation time at 50 and 500 K when using the CHARMM force field. The calculated heat capacity value converges at about 2×10^5 timesteps, and then fluctuates within a 3% range. Thus, the simulation time used (10^6 timesteps) is adequate to obtain accurate heat capacity values.

The quasi-harmonic phonon frequency is obtained from the diagonalization of a weighted fluctuation matrix. Figures 10 and 11 show the comparisons of heat capacity

Table 3. Finite length SWNT phonon frequencies (cm^{-1}).

(10,10) SWNT	*COMPASS*	*Tersoff*	*CHARMM*	*PCFF*	*CVFF*
1	8.1	60.5	19.2	8.16	20.38
2	10.12	61.18	23.48	10.15	24.7
3	25.09	61.4	53	25.28	56.75
4	26.50	62.22	56.2	26.54	59.47
5	46.22	62.39	80.34	45.31	89.74
Highest	1896	2104	1663	1894	2245
(5,5) SWNT	*COMPASS*	*Tersoff*	*CHARMM*	*PCFF*	*CVFF*
1	28.98	87.19	32.4	29.68	38.7
2	29.71	87.2	56.22	30.35	67.8
3	32.21	112.75	57.33	32.49	68.06
4	50.62	113.22	62.87	38	75.54
5	52.92	117.43	72.93	53.62	87.58
Highest	1898	2034	1670	1897	2247

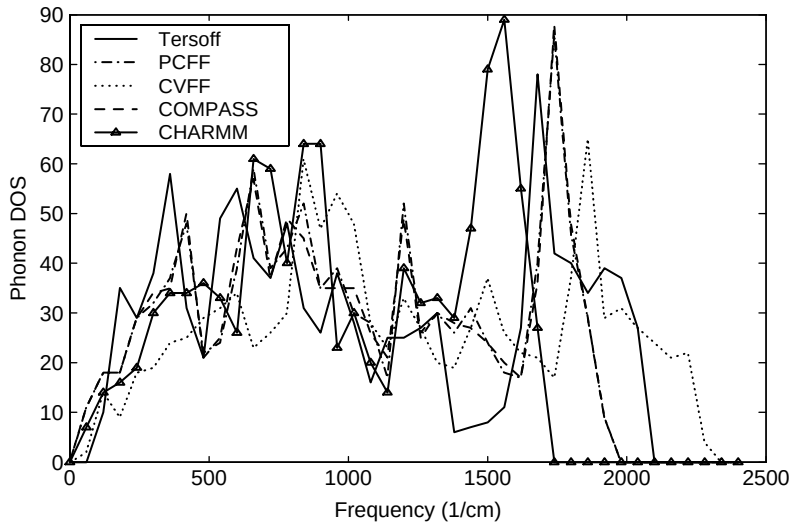

Figure 5. (5,5) Finite length SWNT PDOS.

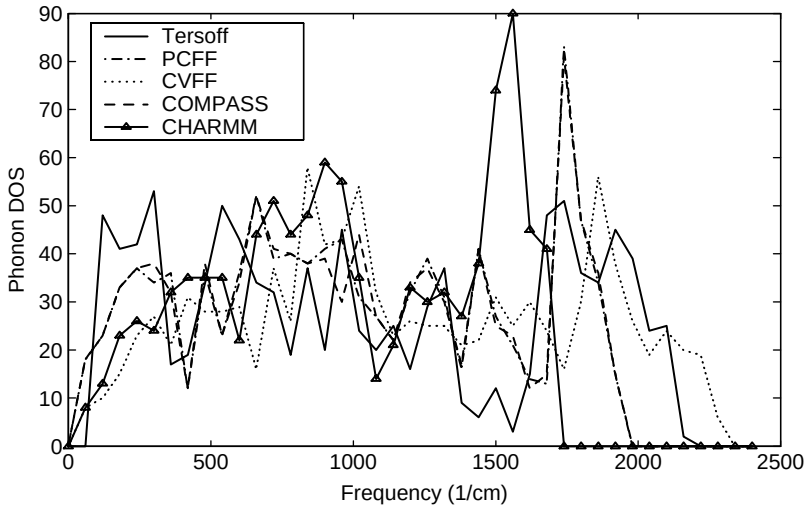

Figure 6. (10,10) Finite length SWNT PDOS.

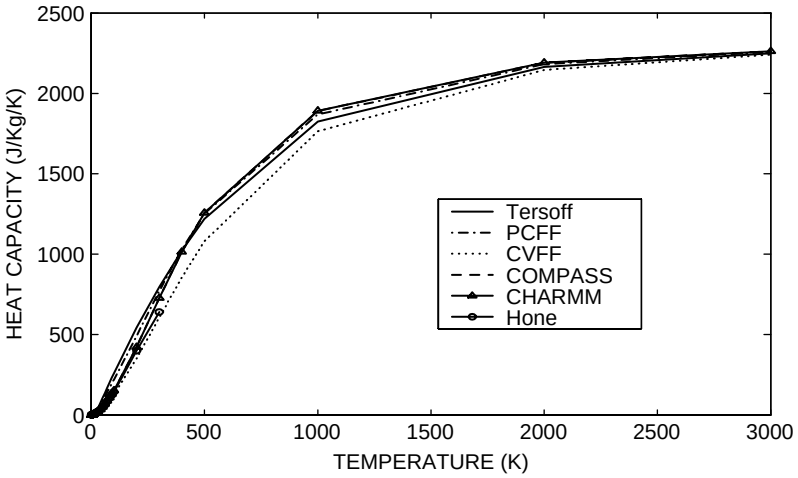

Figure 7. (10,10) Finite length SWNT heat capacity from 0 to 3000 K.

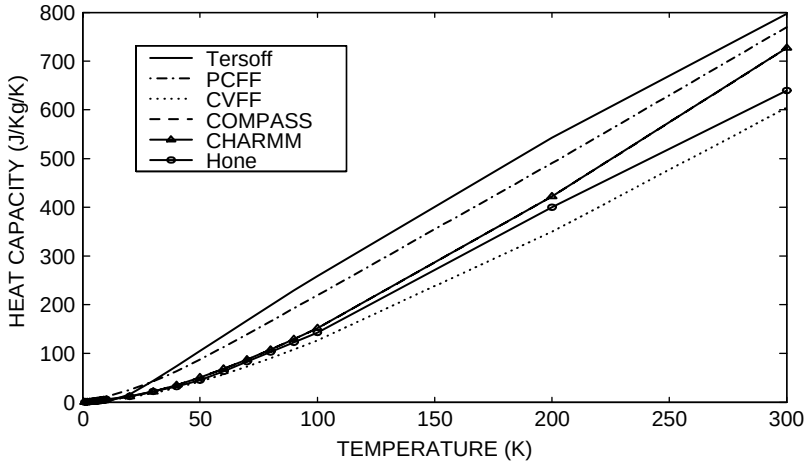

Figure 8. (10,10) Finite length SWNT heat capacity from 0 to 300 K.

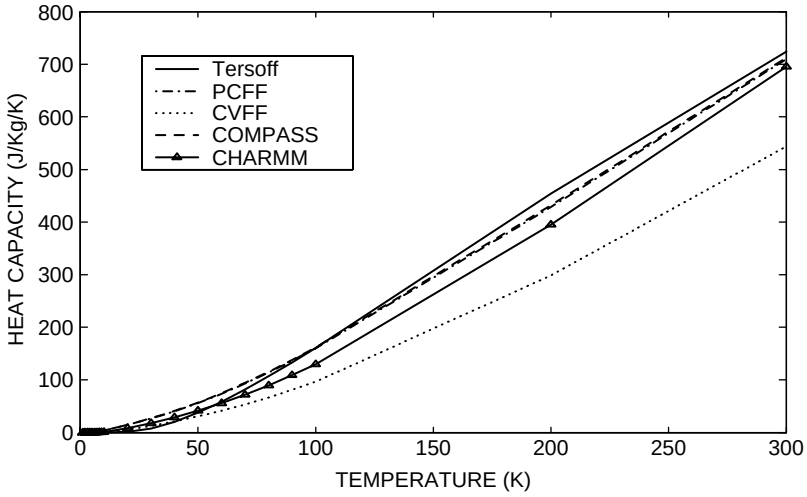

Figure 9. (5,5) Finite length SWNT heat capacity from 0 to 300 K.

results based on the harmonic and quasi-harmonic phonon frequency for the Tersoff and CHARMM force fields for (10,10) finite length SWNTs. The heat capacity from the quasi-harmonic theory is almost the same as that of the harmonic theory at temperatures below 300 K. The deviation in heat capacity between the two methods increases gradually with temperatures above 300 K. At 500 K, $(C_v)_{\mathrm{HA}} = 4831.2$(J/mol/K) and $(C_{\mathrm{vib}})_{\mathrm{QHA}} = 4687.4$ (J/mol/K) for the CHARMM force field, with a difference of -2.98%. For the Tersoff force field, $(C_v)_{\mathrm{HA}} = 4688.5$ (J/mol/K) and $(C_{\mathrm{vib}})_{\mathrm{QHA}} = 4962.0$ (J/mol/K), with a difference of 5.83%. While the heat capacity from the harmonic approximation is overestimated for the Tersoff force field, it is underestimated for the CHARMM force field. In both cases, the deviations are less than 6%, which shows that the harmonic lattice dynamics theory can yield qualitative approximations in the study of the heat capacity of SWNTs at low and intermediate temperatures. The force field comparisons based on the harmonic case in Section 3.1 are valid in the low and medium temperature range.

In figures 10 and 11, the quasi-harmonic results are shown only up to temperature 500 K. The reason for that is that the C—C bond breaking and formation will occur at about 500 K and become more active as temperature

Table 4. Heat capacity (J/mol/K) with simulation time (timestep 1 fs).

Timesteps	10^3	10^4	10^5	2×10^5	10^6	2×10^6
50 K	153.51	153.49	192.74	180.83	175.03	185.50
500 K	781.39	3440.01	4687.43	4742.50	4830.79	4840.70

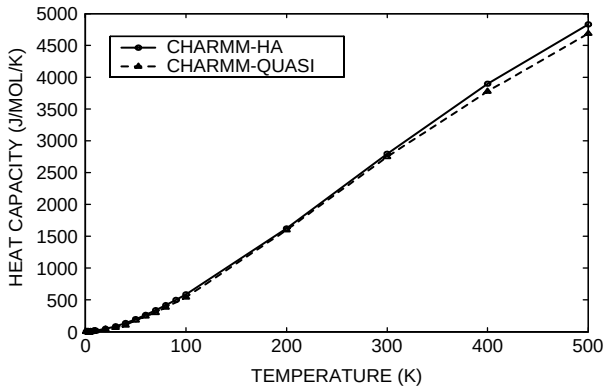

Figure 10. CHARMM force field quasi-harmonic results.

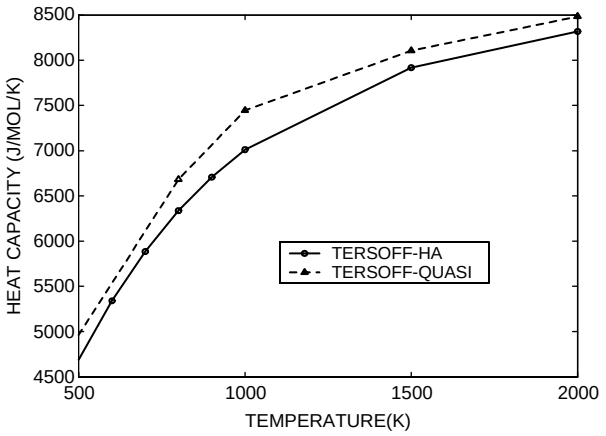

Figure 12. TERSOFF force field quasi-harmonic results beyond 500 K.

increases. The aforementioned force fields are not designed to handle the bond breaking and formation activities.

It is interesting to see the trend from the heat capacity results of both harmonic and quasi-harmonic theory at temperatures above 500 K. The results from the Tersoff force field are shown in figure 12. The quasi-harmonic heat capacity of SWNTs is slightly higher than the harmonic heat capacity in the whole temperature range. The difference between heat capacities from the two theories become larger as the temperature increases, and reaches its maximum at about 1000 K, then becomes progressively smaller at temperatures above 1000 K. This can be explained by the bonding model used with the Tersoff force field. The C—C bond length is stretched longer and the bonding force is weaker as the temperature increases. The quasi-harmonic phonon frequencies of the SWNTs configuration will be lower than the harmonic phonon frequencies. In view of equation (4), this will result in a higher heat capacity value. At very high temperatures (above 2100 K), all bonds are broken, and the carbon atoms are in the gas phase. Results from different theories all converge to the expectation of classical statistical mechanics. Although the current force field can not handle the bond breaking and formation, the heat capacity results shown in figure 12 still capture some of the characteristics of heat capacity above 500 K. Future investigations should use a more appropriate force field such as the second generation Brenner–Tersoff force field [13] in this temperature range.

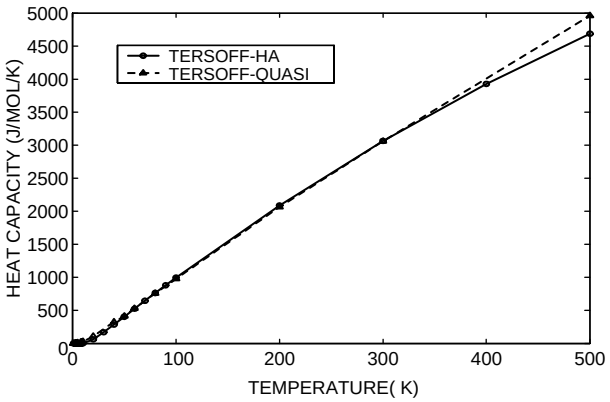

Figure 11. TERSOFF force field quasi-harmonic results.

4. Conclusion

In summary, we calculated the heat capacity of SWNTs using five different force fields. The heat capacity results vary significantly in the low temperature range (below 300 K). Among the tested force fields, the COMPASS force field best reproduces the phonon frequencies calculated from DFT and is consistent with the Raman scattering results. Thus, it gives reasonable results in the computation of the heat capacity of SWNTs, and it is expected to perform well in the prediction of other thermo-mechanical properties. While the Tersoff force field is one of the best for describing the structure and energy properties of the carbon nanotubes, it does not fare as well as the COMPASS force field in the simulation of harmonic heat capacity of SWNTs.

The impact on the SWNT heat capacity from the temperature dependent phonon frequencies is not significant for the low and intermediate temperature range (below 500 K). The force field comparisons based on the harmonic approximation are valid in that temperature range. At temperatures above 500 K, heat capacity results based on Tersoff force field quasi-harmonic approximation were investigated and must be validated by experiment or more accurate force fields in that temperature range.

Acknowledgement

The authors wish to acknowledge the support of the Texas Institute for Intelligent Bio-Nano Materials and Structures for Aerospace Vehicles, funded by NASA Cooperative Agreement No. NCC-1-02038. BMP also thanks the Robert A Welch Foundation for partial support.

References

[1] S. Iijima. Helical microtubules of graphitic carbon. *Nature*, **354**, 56 (1991).

[2] J. Hone, M. Whitney, C. Piskoti, A. Zettl. Thermal conductivity of single-walled carbon nanotubes. *Phys. Rev. B*, **59**, R2514 (1999).

[3] J. Hone, B. Batlogg, Z. Benes, A.T. Johnson, J.E. Fischer. Quantized phonon spectrum of single-wall carbon nanotubes. *Science*, **289**, 1730 (2000).

[4] W. Yi, L. Lu, D.-L. Zhang, Z.W. Pan, S.S. Xie. Linear specific heat of carbon nanotubes. *Phys. Rev. B*, **59**, R9015 (1999).

[5] J.C. Lasjaunias, K. Biljakovic', Z. Benes, J.E. Fischer, P. Monceau. Low-temperature specific heat of single-wall carbon nanotubes. *Phys. Rev. B*, **65**, 113409 (2002).

[6] R. Saito, T. Takeya, T. Kimura. Raman intensity of single-wall carbon nanotubes. *Phys. Rev. B*, **57**, 4145 (1998).

[7] L.J. Porter, J. Li, S. Yip. Atomistic modeling of finite-temperature properties of 3b2-SiC. I. Lattice vibrations, heat capacity, and thermal expansion. *J. Nucl. Mater.*, **246**, 5313 (1997).

[8] A.M. Rao, E. Richter, Shunji Bandow. Diameter-selective Raman scattering From vibrational modes in carbon nanotubes. *Science*, **275**, 187 (1997).

[9] Yu.I. Prylutskyy, S.S. Durov, O.V. Ogloblya, E.V. Buzaneva, P. Scharff. Molecular dynamics simulation of mechanical, vibrational and electronic properties of carbon nanotubes. *Comput. Mater. Sci.*, **17**, p352 (2000).

[10] P. Sokhan, D. Nicholson, N. Quirke. Phonon spectra in model carbon nanotubes. *J. Chem. Phys.*, **113**, 2007 (2000).

[11] M.J. Longhurst, N. Quirke. The radial breathing mode of carbon nanotubes. *Mol. Simul.*, **31**(2/3), 135 (2005).

[12] M.J. Longhurst, N. Quirke. The environmental effect on the radial breathing mode of carbon nanotubes in water. *J. Chem. Phys.*, **124**, 1 (2006).

[13] D.W. Brenner, O.A. Shenderova, J.A. Harrison, S.J. Stuart, B. Ni, S. Sinnott. A second-generation reactive empirical bond order (REBO) potential energy expression for hydrocarbons. *J. Phys.: Condens. Matter*, **14**, 783 (2002).

[14] B.R. Brooks, R.E. Bruccoleri, B.D. Olafson, D.J. States, S. Swaminathan, M. Karplus. CHARMM: a program for macromolecular energy, minimization, and dynamics calculations. *J. Comp. Chem.*, **4**, 187 (1983).

[15] A.D. MacKerrel, *et al.* All-atom empirical potential for molecular modeling and dynamics studies of proteins. *J. Phys. Chem. B*, **102**, 3586 (1998).

[16] A.D. MacKerrel, S.E. Feller. An improved empirical potential energy function for molecular simulations of phospholipids. *J. Phys. Chem. B*, **104**, 7510 (2000).

[17] P. Dauber-Osguthorpe, V.A. Roberts, D.J. Osguthorpe, J. Wolff, M. Genest, A.T. Hagler. Structure and energetics of ligand binding to proteins: *Escherichia coli* dihydrofolate reductase-trimethoprim, a drug-receptor system. *Proteins: Struct. Funct. Bioinf.*, **4**, 31 (1988).

[18] J.R. Maple, T.S. Thacher, U. Dinur, A.T. Hagler. Biosym force field research results in new technique for the extraction of inter- and intramolecular forces. *Chem. Des. Automat. News*, **5**(9), 5 (1990).

[19] H.J. Sun. COMPASS: an *ab initio* force-field optimized for condensed-phase applications-overview with details on alkane and benzene compounds. *Phys. Chem. B*, **102**, 7338 (1998).

[20] H. Sun, P. Ren, J.R. Fried. The COMPASS force field: parameterization and validation for phosphazenes. *Comput. Theor. Polym. Sci.*, **8**(1/2), 229 (1998).

[21] J. Tersoff. Empirical interatomic potential for carbon, with applications to amorphous carbon. *Phys. Rev. Lett.*, **61**, 2879 (1988).

[22] D.W. Brenner. Empirical potential for hydrocarbons for use in simulating the chemical vapor deposition of diamond films. *Phys. Rev. B*, **42**, 9458 (1990).

[23] Material Studio 3.1, www.accelrys.com/doc/life/copyright.html.

[24] M.T. Dove, chapter 5. *Introduction to Lattice Dynamics*, chapter 5. Cambridge University Press, (1993).

[25] R.A. Jishi, L. Venkataraman, M.S. Dresselhaus, G. Dresselhaus. Phonon modes in carbon nanotubules. *Chem. Phys. Lett.*, **209**, 77 (1993).

[26] R.A. Jishi, L. Venkataraman, M.S. Dresselhaus, G. Dresselhaus. Symmetry properties of chiral carbon nanotubes. *Phys. Rev. B*, **51**(11), 176 (1995).

[27] E. Richter, R. Subbaswamy. Theory of size-dependent resonance Raman scattering from carbon nanotubes. *Phys. Rev. Lett.*, **79**, 2738 (1997).

[28] T. Maeda, C. Horie. Phonon modes in single-wall nanotubes with a small diameter. *Physica B*, **479**, 263 (1999).

[29] A. Charlier, E. McRae, M.-F. Charlie, A. Spire, S. Forster. Lattice dynamics study of zigzag and armchair carbon nanotubes. *Phys. Rev. B*, **57**, 6689 (1998).

[30] V.N. Popov, V.E. van Doren, M. Balkanski. Lattice dynamics of single-walled carbon nanotubes. *Phys. Rev. B*, **59**, 8355 (1999).

[31] V.N. Popov. Low-temperature specific heat of nanotube systems. *Phys. Rev. B*, **66**, 153408 (2002).

[32] D. Sa'nchez-Portal, E. Artacho, J.M. Soler, A. Rubio, P. Ordejo'n. *Ab initio* structural, elastic, and vibrational properties of carbon nanotubes. *Phys. Rev. B*, **59**(12), 678 (1999).

[33] L.X. Benedict, S.G. Louie, L. Cohen. Heat capacity of carbon nanotubes. *Solid State Commun.*, **100**, 177 (1996).

[34] S. Nosé. A unified formulation of the constant temperature molecular dynamics methods. *J. Chem. Phys.*, **81**, 511 (1984).

[35] S. Nosé. A molecular dynamics method for simulations in the canonical ensemble. *Mol. Phys.*, **52**, 255 (1984).